Dual-view plane illumination microscopy for rapid and spatially isotropic imaging

Abhishek Kumar[1,2], Yicong Wu[1], Ryan Christensen[1], Panagiotis Chandris[1], William Gandler[3], Evan McCreedy[3], Alexandra Bokinsky[3], Daniel A Colón-Ramos[2], Zhirong Bao[4], Matthew McAuliffe[3], Gary Rondeau[5] & Hari Shroff[1]

[1]Section on High Resolution Optical Imaging, National Institute of Biomedical Imaging and Bioengineering, US National Institutes of Health (NIH), Bethesda, Maryland, USA. [2]Program in Cellular Neuroscience, Neurodegeneration and Repair, Department of Cell Biology, Yale University School of Medicine, New Haven, Connecticut, USA. [3]Biomedical Imaging Research Services Section, Center for Information Technology, NIH, Bethesda, Maryland, USA. [4]Developmental Biology Program, Sloan-Kettering Institute, New York, New York, USA. [5]Applied Scientific Instrumentation, Eugene, Oregon, USA. Correspondence should be addressed to A.K. (abhishk@gmail.com) or H.S. (hari.shroff@nih.gov).

We describe the construction and use of a compact dual-view inverted selective plane illumination microscope (diSPIM) for time-lapse volumetric (4D) imaging of living samples at subcellular resolution. Our protocol enables a biologist with some prior microscopy experience to assemble a diSPIM from commercially available parts, to align optics and test system performance, to prepare samples, and to control hardware and data processing with our software. Unlike existing light sheet microscopy protocols, our method does not require the sample to be embedded in agarose; instead, samples are prepared conventionally on glass coverslips. Tissue culture cells and *Caenorhabditis elegans* embryos are used as examples in this protocol; successful implementation of the protocol results in isotropic resolution and acquisition speeds up to several volumes per s on these samples. Assembling and verifying diSPIM performance takes ~6 d, sample preparation and data acquisition take up to 5 d and postprocessing takes 3–8 h, depending on the size of the data.

INTRODUCTION

Light sheet fluorescence microscopy (LSFM)[1–4] has emerged as a powerful imaging tool for cell and developmental biology. LSFM systems excite the sample with a thin light sheet and collect the resulting fluorescence along a perpendicular detection axis. Imaging volumes are collected by sweeping the light sheet and detection plane through the sample. As only the focal plane is illuminated at any instant, these microscopes provide effective 'optical sectioning' in transparent samples while confining photodamage and bleaching to the vicinity of the focal plane. This is in contrast to confocal microscopy, in which most of the sample volume is illuminated at once and optical sectioning depends on placing a pinhole in the emission path. As a wide-field detector (camera) is used in LSFM to collect information from the entire imaging plane simultaneously, each pixel can be exposed for a much longer duration than in point-scanning microscopes, resulting in images with a very high signal-to-noise ratio (SNR). Collectively, these advantages result in instruments that are much faster, much gentler and which provide images with much better SNRs than laser-scanning confocal microscopy. LSFM has been particularly beneficial in long-term 4D imaging studies, as in the embryogenesis of model organisms such as nematode (*C. elegans*)[5], zebrafish (*Danio rerio*)[6] and fruitfly (*Drosophila melanogaster*)[7,8]. Recent efforts have improved the spatiotemporal resolution of LSFM[9–11] and have enabled the study of fast intracellular dynamics[11] that would have been impossible to capture with other 4D imaging systems.

Modern LSFM systems use one objective lens to deliver the excitation sheet and another to collect the fluorescence. The required perpendicularity between excitation and detection forces the use of relatively long-working-distance objectives and constrains the sample geometry relative to single objective epifluorescence or confocal microscopy. Many LSFM implementations embed the sample in agarose, holding the resultant gel in a capillary tube, which is translated to the focus of a detection objective. By rotating the sample, specimen views acquired at different angles may be fused together into a composite volume, increasing the overall image quality by masking the effects of scattering and light sheet degradation that plague individual views[8]. Moreover, multiview deconvolution can be applied to compensate for the poor axial resolution of any single view by harnessing the much better lateral resolution inherent to a perpendicular view, thereby improving resolution isotropy[12,13]. Detailed protocols that describe the step-by-step assembly and operation of these LSFM systems have recently become available[14,15], making it possible for biologists to build them from commercially available hardware.

Although it is appropriate for large embryos such as *D. rerio* or *D. melanogaster*, embedding a sample in agarose is cumbersome for a large variety of specimens that are more easily grown or deposited on conventional glass coverslips. We and others[16] have designed a version of LSFM that is compatible with glass coverslips: 'inverted selective plane illumination microscopy (iSPIM)'[5]. In iSPIM, two water-dipping objectives that are perpendicular to each other are placed above a sample mounted in a commercially available inverted microscope stand. A light sheet is introduced with one objective and scanned through the sample, and the second objective is translated with a piezoelectric stage (piezo) in order to keep the imaging plane in focus during scanning. The sample can be easily found with a low-magnification objective mounted in the epifluorescence port of the inverted microscope, and it is translated to the focus of each objective. This geometry is well adapted for imaging cultured cells and horizontally mounted tissues, avoiding the difficulty of mounting such samples in a vertical sample holder[17]. More recently, we modified iSPIM to capture a second specimen view, by alternating excitation and

Figure 1 | DiSPIM with major subassemblies.
(**a**) Perspective view of assembled diSPIM,
with microscope frame, inverted microscope
components, cameras and major diSPIM
subassemblies indicated. 'DiSPIM module' refers
to scanners, dichroic filter cubes, tube lenses,
objectives, piezos and associated optomechanics
that move as a single unit on an LS-50
translation stage. Refer to the MATERIALS section
for further description of component parts.
(**b**) Photograph to accompany **a**. (**c**) Higher-
magnification view of excitation and detection
subassemblies in the diSPIM module. Excitation
(blue) and emission (red) along a single arm of
the module are highlighted. (**d**) Detailed view
of the excitation scanner, showing fiber input,
mirrors and relay lenses. (**e**) Higher-magnification
view of objectives, piezos and holders/adjusters.
(**f**) Photograph to accompany **e**. See also
Supplementary Note 1, SF2 and SF3.
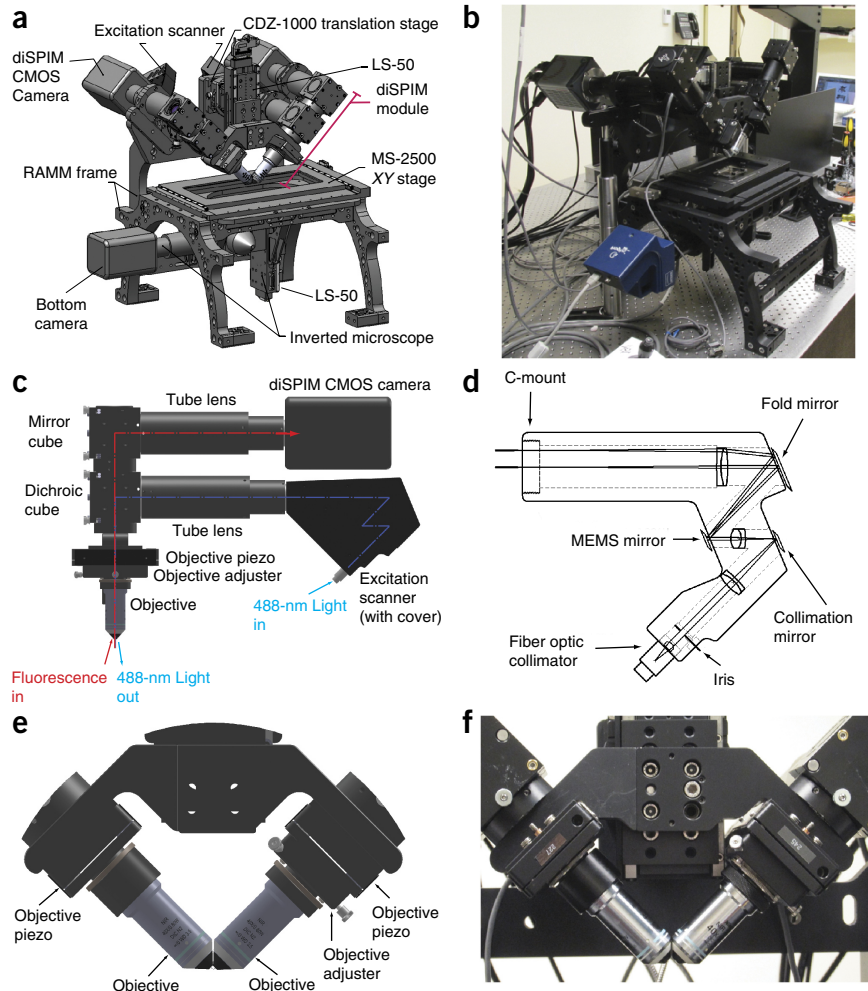
detection between the two objectives.
The resulting 'diSPIM' provides isotropic
spatial resolution (down to 330 nm) at
high speed (200 images per s, 0.5 s for a
dual-view 50-plane volume)[11].

Overview of the procedure

Here we describe the step-by-step
construction of a diSPIM entirely from
commercially available parts (**Fig. 1**).
Unlike our previous implementation[11],
which used free-space optics to couple in
laser excitation to the sample, this design
is compatible with fiber-coupled laser
excitation. Such fiber-based excitation
facilitates alignment, making the device compatible with a broad
array of commercial laser excitation sources, and it assures
collinearity among different excitation wavelengths. Furthermore,
instead of controlling multiple galvanometric mirrors, compact
scan-heads (one for each specimen view) are used to generate
and sweep the excitation sheets through the sample, also aiding
in system alignment. Data acquisition software for generating and
sweeping the light sheets, controlling and synchronizing objec-
tive piezos, and recording images from scientific complementary
metal-oxide semiconductor (sCMOS) cameras is also provided.

After describing diSPIM construction, we present controls for
verifying the spatial resolution of the system and the proper align-
ment of the light sheets. Next, we describe the use of diSPIM in
performing 3D imaging of *C. elegans* embryos throughout 14 h
of development, and imaging of whole cells over ~30 min. The
same protocol can be adapted for 4D studies of other samples
of approximately similar dimensions ($50 \times 50 \times 50~\mu m^3$). We
conclude with the postprocessing (registration and image fusion
and deconvolution) operations necessary to produce data sets
with isotropic resolution.

The procedure is divided into topical subsections. First, general
assembly of the diSPIM is described. This includes setup of the
diSPIM frame and lower imaging path, followed by setup and
alignment of the excitation scanners, dichroic cubes, objectives
and objective piezo assemblies, and cameras (Steps 1–63).
Next, more detailed alignment steps are discussed, including
fine adjustment of the SPIM objectives using visual feedback
from fluorescent beads and dye solution, and fine adjustment of
the field of view (FOV) on the diSPIM cameras (Steps 64–74).
Verification of system alignment, including measurement of
point spread functions (PSFs) and light sheet thickness, is then
described (Steps 75–95). These alignment steps are performed
once while assembling the system, but it is helpful to recheck
the light sheet thickness and PSF once every 2 months. After the
system is built and aligned, we present example protocols for
imaging live samples, such as *C. elegans* embryos and single cells
(Steps 96A and 96B). Finally, we conclude by specifying the data
processing steps used to register and deconvolve the data collected
from fluorescent beads, cells and embryos (Steps 97–106).

Limitations

To obtain the best diSPIM data, it is necessary to obtain high-
quality specimen views from each objective lens. Furthermore,
the objectives must provide faithful but complementary measure-
ments of the same object. If the object moves during dual-view
acquisition (motion blur), if one view provides noticeably inferior
image quality (owing to depth-dependent scattering or aberra-
tions that preferentially degrade that view), or if the two views

are poorly aligned, the fused reconstruction may display artifacts (**Supplementary Note 1**, SF1 and **Supplementary Data 1**). In extreme cases, the registration algorithm may be unable to correctly align the two views owing to a low degree of similarity between the views. Although we prefer dual-view acquisition owing to the isotropic resolution it provides, we note that single-view operation (iSPIM[5]) is at least twice as fast and may be preferred if acquisition speed is of paramount importance. Single-view operation also obviates imaging artifacts that arise because of the registration or fusion process, and it is fully compatible with this protocol.

We have enjoyed the most success when imaging small (~50–60 μm), transparent samples (single cells, a few layers of cells or *C. elegans* embryos; **Supplementary Videos 1** and **2**), wherein the 3D dynamics of interest occur no faster than several volumes per s. Larger samples may be accommodated by using lower-magnification objectives (10× or 20× lenses) and/or by widening the width of the light sheet (by further stopping down the iris)—although we do not cover this explicitly in this protocol, our design is flexible enough to accommodate such changes (**Supplementary Table 1**). For especially large, scattering samples (such as *D. melanogaster* embryos), two-photon excitation may provide better performance than conventional single-photon excitation[18]. In this case, modifications to our system might include fibers appropriate for the high pulsed intensities generated by femtosecond laser sources, optical components that are better adapted for near-IR wavelengths and alternate methods of shuttering or modulating the beam intensity. Implementing confocal slit detection[19] in each arm would also reduce background in scattering samples. Finally, we note that alternative LSFM implementations that use bidirectional illumination[18] and detection[7,8] may offer better sample coverage in large specimens than the implementation we describe here.

Experimental design

Fiber-coupled laser excitation. The laser excitation in this design is coupled to the diSPIM module by two optical fibers, one for each arm of the microscope. Many commercial options exist for single-mode fiber-coupled laser excitation (for example, the Nikon MLC 400B), providing compact assemblies with a range of wavelengths and powers (~10 mW per laser line at the output of each fiber is more than sufficient for most fluorescent samples). If you are obtaining a commercial solution, the two requirements are: (i) the end of the fiber should have an FC/PC (or FC/APC) connector, for coupling into the diSPIM excitation scanner; and (ii) it should be capable of rapidly modulating the power and switch between laser lines at high speed (ms or faster).

A cheaper, but potentially more time-consuming, option is to construct your own laser launch from component parts. Although the step-by-step construction of such an assembly is outside the scope of this paper, we provide a schematic and photograph of our custom-built diSPIM launch (**Supplementary Note 1**, SF2). In this setup, we use an acousto-optic tunable filter (AOTF) to modulate 488-nm (for exciting GFP and similar fluorophores) and 561-nm (for exciting mCherry and similar fluorophores) laser wavelengths, combining the two lines before splitting the beams into two optical fibers. The maximum power at the fiber output (before insertion into the diSPIM scanners) in this design is 20 mW (488-nm excitation) and 10 mW (561-nm excitation).

Microscope hardware. The major components of the diSPIM are shown in **Figure 1** and **Supplementary Note 1**, SF3. The microscope is assembled on a rapid automated modular microscope (RAMM) frame (**Fig. 1a,b**). DiSPIM functionality is provided by a 'module' (**Fig. 1c**) that is mounted above the sample stage. This module combines excitation (via scanner assemblies that accept fiber input and create the light sheets, **Fig. 1d**, described in greater detail in the 'Excitation scanners' subsection below), holders for dichroic mirrors, conventional mirrors and emission filters, piezoelectric stages that translate objectives (**Fig. 1e,f**) and various adjusters that aid in system alignment. Once assembled, the diSPIM module moves as a single unit vertically, allowing the light sheets to be positioned arbitrarily within the sample without disrupting the alignment. As diSPIM requires two perpendicular specimen views, the diSPIM module is highly symmetric (**Fig. 1e,f**), with each 'arm' of the module (**Supplementary Note 1**, SF3) containing all hardware necessary for providing laser excitation and fluorescence detection. These arms are referred to below as 'arm A' and 'arm B'. High-speed sCMOS cameras (one for each arm) are mounted to the optical table independently of the diSPIM module (**Supplementary Note 1**, SF3), minimizing the coupling of vibrations induced by the camera fans to the rest of the system. We also equip the conventional (lower) imaging path of the RAMM with a low-magnification objective and automated *XY* stage (**Fig. 1a,b**), thus allowing us to rapidly locate and position samples for diSPIM. We note that, although we do not describe the functionality in detail here, the lower imaging path can also be used for epifluorescence imaging.

Several hardware components are moved during system alignment or data acquisition. The low-magnification 10× objective used in finding the sample and the diSPIM module are each mounted on an LS-50 automated translation stage, enabling coarse focusing (for the objective) or positioning (for the diSPIM module). The use of the stage controller supplied with the diSPIM frame allows the user to toggle between each stage (the LS-50 stage used in controlling the low magnification objective is assigned the '*Z*' axis and the LS-50 stage used in controlling the diSPIM module's height is assigned the '*F*' axis; refer to the Applied Scientific Instrumentation (ASI) manual for more documentation on these controls). Microelectromechanical systems (MEMS) 2D mirrors, mounted in each arm of the diSPIM module, scan the fiber excitation in one direction to create a light sheet and in a perpendicular direction to sweep the sheet through the imaging volume. Finally, objective piezos are scanned during volumetric image acquisition after being aligned and synchronized with the light sheets by applying analog voltages to each piezo (applying a voltage of 0.05 V corresponds to a 1-μm movement of the 200-μm travel range piezo).

Excitation scanners. The ASI scanners used in each arm are compact and versatile scan-head units that were designed specifically for generating the illumination used in light sheet microscopy. These integrated 2D MEMS mirrors provide lightweight, low-vibration optical scanning of light from a single-mode fiber-coupled laser. The basic design of the unit consists of a series of 4f lens pair arrangements with the scan mirrors, apertures and focal planes located at the foci of the lenses (**Fig. 1d**).

The input to the scanner is a fiber collimator that accepts a single-mode FC/PC (or optionally FC/APC)-connected

PROTOCOL

fiber-coupled laser source. The fiber collimator is an exchangeable part that allows some flexibility in the focal length, and hence intrinsic beam diameter, and in the fiber connector type. The collimated laser beam can be stopped down with the iris diaphragm if desired, thereby creating light sheets with different thicknesses that are suitable for samples of varying size (**Supplementary Table 1**). The collimated laser is focused onto the first fold mirror ('collimation mirror' in **Fig. 1d**). Translating the axial position of this mirror changes the collimation state of the beam as it emerges from the scanner. After reflecting from the first fold mirror, the focused light is collimated again and projected onto the 2D MEMS scanner mirror. The plane of the scan mirror is conjugate to the microscope objective's back focal plane. Tilting the scan mirror thus steers the focused laser beam to different positions in the sample focus plane. For diSPIM applications, the tube lens is positioned to recollimate light at the objective back focal plane so that the focused laser beam remains parallel to the optical axis when scanning off-axis.

To use the scanners to create and sweep light sheets through the sample, we apply analog voltages to each axis of the MEMS mirrors. For the scanners and optics used in this protocol, 1 V applied to the MEMS mirror produces a 1.6° angular change (mechanical), which corresponds to an 80-μm displacement in the sample.

Data acquisition. We use the LabVIEW programming environment to synchronize cameras, excitation scanners, objective piezos and laser excitation. All .vi programs (.vi is the extension appended to LabVIEW virtual instrument programs) are available at http://www.wormguides.org/dispim/dispim-downloads, where they will be regularly updated. The three main .vi programs that we use are: (i) Camera Test.vi, used for checking the performance of the Hamamatsu Flash 4.0 sCMOS cameras; (ii) diSPIM Control.vi, used for controlling the diSPIM during image acquisition; and (iii) Tiff Conversion.vi, used for converting the Hamamatsu image file format into .tif format. **Supplementary Note 2** describes these programs in detail.

Data processing. After acquisition, the volumes acquired in each view must be processed (spatially registered, fused and deconvolved)[11] to yield images with isotropic resolution. All of these operations are now implemented as a plug-in in the open-source MIPAV (medical image processing, analysis and visualization) programming environment (http://mipav.cit.nih.gov/)[20]. The latest version of this software is compatible with a graphics processing unit (GPU) card (**Supplementary Table 2**), thereby improving the speed of joint deconvolution tenfold relative to our previous work (for imaging volumes of size $260 \times 360 \times 50$ pixels, the GPU-based plug-in can process 6 volumes/min).

MATERIALS

REAGENTS
For verifying diSPIM alignment and system performance
- Alexa Fluor 488 fluorescent streptavidin (Invitrogen, cat. no. S-32354)
- Yellow-green fluorescent beads, 100 nm (Invitrogen, cat. no. F8803)

For *C. elegans* embryo imaging
- Gravid young adult *C. elegans*, strain BV24 [ltIs44 [pie-1p-mCherry:: PH(PLC1delta1) + unc-119(+)]; zuIs178 [(his-72 1 kb::HIS-72::GFP); unc-119(+)] V], as described in Wu *et al.*[5]
- Poly-ʟ-lysine (Sigma-Aldrich, cat. no. P1524)
- Methyl cellulose (Sigma-Aldrich, cat. no. H7509-25G)
- M9 buffer, see Stiernagle[21]

For cellular imaging
- DMEM with high glucose (4.5 g/l), supplemented with GlutaMAX and sodium pyruvate (Life Sciences, cat. no. 10569-069)
- DMEM without glucose, glutamine, pyruvate and phenol red (Life Technologies, cat. no. A14430-01)
- Glucose solution, 45% (wt/vol) (Corning, cat. no. 25-037-CI)
- Sodium pyruvate, 100 mM (Life Technologies, cat. no. 11360088)
- GlutaMAX supplement (Life Technologies, cat. no. 35050061)
- Sodium bicarbonate, 7.5% (wt/vol) solution (Life Technologies, cat. no. 25080094)
- HyClone FBS, defined (Thermo Scientific, cat. no. SH30070.03)
- HEPES 1 M sterile-filtered solution, pH 7.0–7.6 (Sigma, cat. no. H0887)
- TurboFect transfection reagent (Thermo Scientific, cat. no. R0531)
- Tissue culture dish, 100 mm, BD PureCoat amine (BD, cat. no. 354732)
- Hydrochloric acid (HCl), 37% (wt/vol) solution (Sigma, cat. no. 320331)
- Ethanol, 99.5% (vol/vol; Sigma, cat. no. 459844)
- GFP-tagged H-Ras plasmid[22] (GenBank accession no. AF493916)
- Transformed human lung fibroblasts[22]
- Glass coverslips, no. 1.5, 24 × 50 mm (VWR International, cat. no. 48393-241)

EQUIPMENT
For diSPIM system
- diSPIM acquisition and data processing computer workstation (HP, cat. no. Z820 with features and accessories described in **Supplementary Table 2**). This computer should also include a solid-state RAID drive, with specifications equivalent or similar to

the following: Corsair Neutron Series GTX, solid state drive—240 GB— internal—2.5-inch—SATA-600—buffer: 128 MB, quantity 4; LSI Mega-RAID SAS 9261-8i, storage controller (RAID)—8 channel—SATA 6 Gb/s; SAS low profile–600 Mbps—RAID 0, 1, 5, 6, 10, 50, 60—PCIe 2.0 ×8
- ICY DOCK MB882SP-1S-1B 2.5–3.5-inch SATA 6 Gb SSD and hard drive converter
- DiSPIM optomechanical components, including RAMM base, excitation scanners, bottom imaging path, all mounting accessories, stages and imaging chamber (ASI, described fully in **Supplementary Table 3**)
- O-ring for imaging chamber (O-Rings West, cat. no. M1.5X40)
- Excitation laser launch (Nikon MLC 400B), providing fiber-coupled 488- and 561-nm excitation (or build your own; **Supplementary Note 1**, SF2)
- Data acquisition card chassis (National Instruments, cat. no. PXIe-1073)
- Data acquisition cards (DAQ), quantity 2 (National Instruments, cat. no. PXI-6733)
- Shielded Bayonet Neill-Concelman (BNC) connector block, quantity 2 (National Instruments, cat. no. BNC-2110)
- BNC cables, 4 and 10 feet, quantity 10 each, (L-Com, cat. nos. CC58C-4 and CC58C-10)
- Shielded connector cables, quantity 2 (National Instruments, cat. no. SH68-68-EP)
- Dichroic mirrors for SPIM imaging, 2 mm thick, quantity 2 (Chroma, cat. no. ZT405/488/561/IR RPC)
- Fluorescence emission filters for SPIM and imaging through bottom path, quantity 3 each (Semrock, 488 nm long-pass filter, cat. no. LP02-488 RU-25 and 561-nm notch filter, cat. no. NF03-561E-25)
- DiSPIM ×40, 0.8 numerical aperture (NA), water dipping objectives, quantity 2. (Nikon, cat. no. MRD07420)
- ×10, 0.3 numerical aperture air objective for finding samples via bottom imaging path (Olympus, cat. no. 1-U2B524)
- SPIM detection camera, quantity 2 (Hamamatsu, Flash 4.0)
- Bottom imaging path detection camera (Jenoptik, Jenoptik ProgRes MF CCD microscope camera)
- DiSPIM camera mount optomechanics (Thorlabs, quantity 8, 4-inch mounting posts, cat. no. P4-1.5; quantity 4, studded pedestal base adaptor, cat. no. PB4; quantity 4, clamping fork for 1.5-inch post, cat. no. PF-175; quantity 2, 1/2-inch diameter (length 4 inches) post holder, cat. no. PH4;

quantity 4, 1/2-inch diameter (length 4 inches) stainless steel optical post, cat. no. TR4)
- Optical table with isolators, 4 feet × 6 feet × 12 inches (TMC, cat. nos. 784-651-02DR and 14-416-34)
- Metric and imperial ball-drivers and hex keys for bolting and unbolting optomechanical components (Thorlabs, cat. nos. TC2, TC3/M)

For testing equipment
- Oscilloscope for checking data acquisition signals (Tektronix, cat. no. DPO 2004B)
- Power meter and photodiode power sensor for checking excitation power (Thorlabs, cat. nos. PM100D and S121C)

Software for running diSPIM
- LabVIEW 2011, 64 bit (National Instruments)
- National Instruments drivers for DAQ cards (http://joule.ni.com/nidu/cds/view/p/id/3802/lang/en)
- Hamamatsu DCAM-API driver for SPIM cameras (http://dcam-api.com/downloads/)
- Hamamatsu LabVIEW vis for running Flash 4.0 cameras (video capture library; http://dcam-api.com/hamamatsu-software/)
- HCIMG software from Hamamatsu to control the Flash 4.0 cameras
- ASI LabVIEW vis (http://www.asiimaging.com/support/downloads/ms-2000-control-using-nis-labview-and-the-serial-port/)
- ProgRes CapturePro camera control software for bottom camera

Software for analyzing and processing data
- ImageJ, 64-bit version (http://rsbweb.nih.gov/ij/)
- MIPAV (http://mipav.cit.nih.gov/), 64 bit, version 7.1.0

For *C. elegans* embryo imaging
- Square watch glass (Carolina Biological Supply Company, cat. no. 742300)
- Stainless steel scalpel blade (Feather safety razor, no. 15 blade)
- Scalpel handle (Feather safety razor, no. 3 handle)
- Microcapillary pipette aspirator tube (Sigma-Aldrich, cat. no. A5177)
- Microcapillary pipettes, 0.4-mm i.d. (Drummond Scientific, cat. no. 1-000-800)
- Glass coverslips, no. 1.5, 24 × 50 mm (VWR International, cat. no. 48393-241)
- Dissecting microscope with 10×–50× zoom range and fluorescence capability (for example, Leica, cat. no. MZ10F)
- Platinum wire, 0.5-mm diameter (Sigma-Aldrich, cat. no. 267201)
- Pasteur pipette (Corning/Sigma-Aldrich, cat. no. CLS7095D5X)

REAGENT SETUP
M9 buffer M9 buffer for imaging worm embryos is prepared as described in Stiernagle[21]. M9 buffer can be stored at 23 °C for 6–8 weeks.
Poly-L-lysine Poly-L-lysine is used for sticking the embryos to glass coverslips. We use a working concentration of 1 mg/ml Poly-L-lysine dissolved in Milli-Q or similarly clean water. For long-term storage, prepare 5–10-ml aliquots and store them at −20 °C. Once thawed, the aliquots can be stored at room temperature (23 °C) indefinitely.
Methyl cellulose Methyl cellulose is used for cutting the worms in order to release the embryos. Prepare a 1% (wt/vol) solution in M9 buffer (we usually prepare 50-ml batches containing 0.5 g of methyl cellulose). Methyl cellulose

must be stirred in warm M9 until it is dissolved. Once prepared, this solution can be stored at room temperature for up to 6 months.
Preparation of coverslips with fluorescent bead layer Fluorescent beads are convenient resolution targets, and they are useful in aligning and testing the diSPIM. Pipette 50 μl of poly-L-lysine onto a cleaned coverslip, by smearing it across the central region. After letting the solution dry for 5 min and pipetting off excess poly-L-lysine, add 50 μl of 2,000×-diluted 100-nm yellow-green bead solution. Allow the beads to dry completely, and wash them two or three times with water. Coverslips can be stored indefinitely at room temperature.
Dye solution Dye solution is useful to visualize the fluorescent emissions from the light sheets during diSPIM alignment. We usually start by diluting Alexa Fluor 488 streptavidin conjugate 1,000× in water (this solution can be stored at room temperature over a period of weeks), adjusting the concentration as necessary during imaging.
EQUIPMENT SETUP
Worm-pick creation Worm picks for gathering and moving gravid *C. elegans* are made by inserting a 32–38-mm platinum wire into the thin end of a glass Pasteur pipette, so that roughly 20 mm of the wire protrudes from the pipette. The end of the pipette is briefly heated over an ethanol lamp to fuse the glass to the platinum wire. After fusing, pliers are used to flatten the end of the platinum wire, thus increasing the available surface area for picking worms. Note that this procedure is covered in great detail in Murray and Bao[23].
Mounting coverslips into the imaging chamber The samples in the following procedure need to be mounted on cleaned (as described previously[24]) rectangular coverslips that are then placed into the steel imaging chamber. This procedure usually takes 5–10 min, and it must be done carefully in order to avoid cracking the coverslip. First, a small square (5 mm on a side) is drawn on the center (and underside) of the coverslip with a Sharpie or similar pen. An O-ring is placed in the top half of the chamber, and the coverslip is placed between the upper and lower parts of the chamber (**Supplementary Note 1**, SF4). The two halves are then screwed together. Some practice is necessary to make the chamber watertight without cracking the coverslip (which usually results from overtightening the screws). Finally, 20–40 μl of poly-L-lysine is added to the square in the middle of the coverslip and allowed to dry for 5 min before adding the buffer and sample to the coverslip.
Sharp microcapillary pipette for aspirator tube The pipette is used for transferring embryos. First, hold a microcapillary pipette at both ends. Heat the pipette over the flame of an ethanol lamp or Bunsen burner until the glass softens. Once the glass is soft, quickly pull the pipette out of the flame while simultaneously pulling the ends of the pipette apart. This should create a very narrow tip. Gently break the pipette tip on a tabletop or other nearby surface, if necessary using a razor blade to remove the pipette tip. Once the tip is broken off, the pipette can be used in an aspirator tube (mouth pipette) to transfer the embryos.

PROCEDURE
Setting up the optical table, computer, excitation laser sled and testing cameras ● TIMING 2 d
▲ **CRITICAL** Steps 1–95 cover microscope assembly and performance characterization, and they are done only for the initial setup. Steps 96–106 cover routine imaging of cells and embryos and associated image processing.

1| Install and float the optical table according to the manufacturer's instructions. Position the computer next to the optical table.
! CAUTION Optical table components are extremely heavy. Consider getting professional movers to help with installation.

2| Install the data acquisition (DAQ) card in the computer, and connect the chassis to the DAQ card.

3| Plug in the computer and install the software in the order listed in the MATERIALS section above.

4| Connect the BNC connector blocks to the DAQ card chassis.

PROTOCOL

5| Test all analog output channels from the BNC connector block using the National Instruments Measurement and Automation Explorer software (included with LabVIEW) and the oscilloscope.

6| Install the Hamamatsu camera link cards in the computer.

7| Attach cameras using the manufacturer-supplied cables, and switch on both cameras (as described in the Flash 4.0 manual).

8| Test the performance of the cameras using 'Camera test.vi' (a detailed description of all .vi files is provided in **Supplementary Note 2**).

9| Install the excitation laser launch. If you are using a commercial unit, determine how the laser lines can be controlled with analog voltages. Make the necessary electronic connections to provide analog voltages to the commercial laser launch from the DAQ cards. If you are using a home-built laser launch, control the lasers using the AOTF. Connect the AOTF controller to the DAQ cards with BNC cables. Verify that all laser lines can be shuttered and that their intensity can be varied using the AOTF controller.
! CAUTION To avoid serious injury when using lasers, always follow recommended safety procedures. We recommend the use of laser warning signs and safety equipment (such as laser goggles) in line with requirements set by institutional, local and national safety standards.

10| Connect and test the bottom camera using the manufacturer-supplied camera control software.

Setting up the diSPIM frame and installing the lower imaging path ● TIMING 4–6 h
11| Bolt the RAMM frame to the optical table.

12| Attach the bottom LS-50 stage.

13| Attach the mirror cube to the LS-50 stage.

14| Insert emission filters (488-nm long-pass and 561-nm notch filters) into the dichroic filter cube, and then attach the dichroic filter cube to the mirror cube.

15| Slide the tube lens through the bracket and lock it onto the dichroic filter cube.

16| Attach the bottom camera to the tube lens using the c-mount connection.

17| Attach the 10× objective to the objective adaptor on the LS-50 stage (components in the bottom imaging path are shown in **Supplementary Note 1**, SF3).

18| Install the *XY* sample stage on the RAMM frame and connect cables to the stage controller. Confirm that the *XY* stage is operational using the joystick. Connect both motorized LS-50 translation stages (the first holding the bottom objective and the second holding the diSPIM module) to the stage controller. Note that the LS-50 holding the bottom objective is identified as 'axis ID Z' and the diSPIM module is identified as 'axis ID F' (see ASI manual for more detail). The cables for connecting the stages are labeled accordingly.

19| Move the bottom objective up and down using the knob provided in the stage controller.
▲ CRITICAL STEP For the bottom objective, moving up signifies moving toward the coverslip, and moving down signifies moving away from the coverslip.

20| Focus the bottom objective on a marked coverslip. Mark a black dot (using a Sharpie or similar pen) in the center of a cleaned coverslip. Place the coverslip in the sample chamber (**Supplementary Note 1**, SF4) and mount the chamber on the stage. Make sure that the marked surface is facing up. Turn on the room lights and focus the bottom objective on the coverslip. Locate the black mark on the coverslip and position it in the center of the FOV of the bottom camera. Focus the bottom objective on the black mark using visual feedback from the camera (focusing at the edge of the mark may be easier than focusing in the center; use exposure time: 300 ms). Record the *XY* position of the stage and the position of the bottom objective displayed on the stage controller.

Aligning the excitation scanners ● TIMING 3–4 h

21| Connect the fiber output from the laser launch to each scanner. Turn on the 488-nm laser output and project both beams onto a wall or board, which is at least 1 m away from the scanner.

22| Ensure centration of beams on each MEMS mirror (**Supplementary Fig. 1**). If the beams are not centered, use the MEMS mirror adjusters (the four screws holding each MEMS mirror) to improve centration.

23| Once the beams are centered, open and close the iris and monitor the output beams. Close the iris so that the MEMS mirror boundary is not visible in the beam profile. (This ensures that the beam diameter is not bigger than the MEMS mirror.) ▲ CRITICAL STEP Do not close the iris completely, as this affects the light sheet thickness (**Supplementary Table 1**) and reduces excitation power.

24| Switch off the 488-nm laser, attach the tube lens to the scanner and mount both scanner assemblies on an optical table using tube lens brackets and posts (**Supplementary Fig. 1**). Switch on the 488-nm laser and examine the collimation of each beam. The beams should not markedly change their diameters (i.e., they should be well collimated) over a distance of at least 5 m, and they should emerge from the center of the tube lenses (using a circular target is helpful in checking centration after the tube lenses; **Supplementary Fig. 1**). If the beam diameter noticeably grows or shrinks over this distance, the beam collimation state must be adjusted by translating the position of the collimation mirror (**Fig. 1d**). Once both beams are collimated, remove the tube lens and check the centering of each beam on its MEMS mirror again (Step 22). If the beam is not centered, repeat Steps 22–24 and recheck the collimation. Repeat this process until both beams are well centered and collimated.

Assembling the optics in dichroic filter cube holders and attaching them to excitation scanners ● TIMING 1 h

25| Remove the top plate of the dichroic filter cube holder along with the dichroic filter cube (refer to **Supplementary Note 1**, SF5). Release the dichroic filter cube by loosening the screw on the top plate.

26| Open the dichroic filter cube and slide in the dichroic mirror.
▲ CRITICAL STEP Make sure that the reflecting surface of the dichroic mirror faces the laser input. Do not overtighten the screws holding the dichroic mirror in place, as this will cause optical aberrations.

27| Insert the emission filters (488-nm long-pass and 561-nm notch filters) on the transmission side of each dichroic filter cube. Reattach the dichroic filter cube to the top plate and mount it in the dichroic filter cube holder. Repeat Steps 25–27 for each SPIM arm.

28| Attach scanners to the dichroic filter cube holders (**Supplementary Note 1**, SF6).

29| Switch on the 488-nm laser beams for both SPIM arms, ensuring that the beams emerge straight through each aperture and intersect above the *XY* stage (**Supplementary Note 1**, SF7). If the beams are not intersecting, refer to the Troubleshooting table.
? TROUBLESHOOTING

Assembling the objective piezo assemblies and coarsely aligning SPIM objectives ● TIMING 1 d

30| Attach the objective piezos to each SPIM arm.

31| Mount the objective adjuster on SPIM arm B.

32| Attach the objectives to each arm.

33| Adjust the position of the objectives along their respective optic axes. Move the objectives in and out by loosening the metal ring that holds the objective holder to the piezo. Bring both objectives to within ~0.7 mm (**Supplementary Note 1**, SF8), and make sure that they are at the same height (visual inspection is sufficient at this point).

34| Switch on the 488-nm laser and visually inspect the beams emerging from the objectives. Make sure that beams emerge from the center of each objective. If the beams are not centered, or they obviously emerge at an angle from the objective optic axis, adjust the tilt of the dichroic mirrors in each arm until they are centered (using the three screws on the top plate of the dichroic filter cube; **Supplementary Note 1**, SF5).
▲ CRITICAL STEP If beams are not centered, they will not emerge at 45° to the optic axis of the bottom objective.

35| Repeat Step 34 until both objectives are at the same height, ~0.7 mm apart (**Supplementary Note 1**, SF8) and the beams emerging from each objective are centered.

36| Remount the marked coverslip from Step 20 onto the sample chamber, fill the chamber with water and place the chamber onto the stage.

37| Connect the piezo cables to the Tiger controller.

38| Connect the Tiger controller inputs to the DAQ cards (BNC extension boards) using BNC cables, as described in **Supplementary Note 2**.
▲ **CRITICAL STEP** Unplug the power cable of the Tiger controller before connecting the inputs to the DAQ card.

39| Open 'diSPIM Control.vi' (**Supplementary Note 2**) and select parameter adjustment mode. Enter the following parameters: Time/Plane, 1,000; *Z* Step Size, 0; Planes/Volume, 0; Light Sheet Width, 0; no. of Volumes, 1; Time Point Delay, 0; SPIM arm A and B *Z*-Galvo offset, 2.5 V; *Y*-Galvo offset, 2.5 V; Objective offset, 5 V; *Z*-Galvo and Piezo Conversion factor, 0. Here '*X, Y* and *Z*' are local coordinates that refer to the individual excitation, defined in **Supplementary Note 2**.

40| Switch on the Tiger controller and run 'diSPIM Control.vi'. This will bring the objective piezos to the center of their range by providing an offset voltage of 5 V. It will also move the MEMS mirror to the zero position in both arms.
▲ **CRITICAL STEP** It is prudent to monitor the output of the piezos using an oscilloscope. Connect the 'sensor out' signal from the piezo card to the oscilloscope, and ensure that the sensor readout displayed on the oscilloscope matches the voltage applied to the piezo. If inconsistencies are observed, contact ASI.

41| Bring the diSPIM module down (toward the coverslip) using the stage controller and ensure that the objectives do not touch the coverslip.
▲ **CRITICAL STEP** Move the diSPIM module in small (~10 μm) steps to ensure that the objectives do not hit the side walls of the chamber.

42| Stop moving the diSPIM module toward the coverslip once the intersection of the two beams touches the coverslip surface (visual inspection is enough at this point).

43| If the intersection of beams is laterally offset from the black mark, adjust the position of the CDZ-1000 stage (**Supplementary Note 1**, SF9) until the beams intersect each other on the black mark. Record the *F* axis position from the stage controller.

44| Move the diSPIM module as far away from the coverslip as possible (~35 mm), remove the imaging chamber, replace the marked coverslip with a fluorescent bead sample and place the imaging chamber back in the diSPIM. Bring the diSPIM module toward the coverslip at the *F* axis position recorded in Step 43, and examine the resulting fluorescence through the bottom camera, using an exposure time of 300 ms.

45| Add 10 μl of undiluted dye solution to the chamber. Two beams should be visible in the bottom camera, corresponding to the excitation from each SPIM arm. These beams should form 'spots' near the coverslip surface (an example image is presented in **Supplementary Fig. 2**).

46| If the spots do not overlap, attempt to bring them closer using the objective adjuster and by moving the diSPIM module toward or away from the coverslip (in 5–10-μm steps). Both spots should be as focused as possible, as viewed in the bottom camera, and they should overlap completely (as shown in **Supplementary Fig. 2**). Record the *F* axis position once the spots overlap and the focus has been optimized.
▲ **CRITICAL STEP** Do not attempt to focus by using the lower objective; the goal is to bring the spots to the focal position determined in Step 20.

47| Once the spots in the bottom camera overlap, refocus the bottom objective and compare their relative sizes (if the spots are very bright and saturate the camera pixels, reduce the laser power). If they are not of the same size, repeat Steps 33 and 34 until the spots are equal in size (the difference should not be >20%).

48| Expect to iterate Steps 33–47 until the two spots are separated by no more than 50 μm, as viewed in the bottom camera, and they appear to be of the same size. This might take several hours.

Assembling and positioning the SPIM cameras ● TIMING 4–5 h
49| Bring the diSPIM module to the *F* axis position recorded in Step 46.

50| Attach 65-mm spacer tubes to each dichroic filter cube holder (**Supplementary Note 1**, SF10).

51| Attach the mirror cube holders to the spacer tubes so that the circular opening in the cube points toward the back of the microscope.

52| Attach the tube lenses to the SPIM cameras.

53| Place the SPIM cameras in a horizontal position so that the bottom plate faces down, toward the optical table (the bottom plate of each Flash 4.0 camera has four threaded holes that are a convenient reference point, **Supplementary Note 1**, SF11).

54| Mount the tube lenses into the brackets and mount the brackets onto variable height posts (**Supplementary Note 1**, SF3; posts are assembled by screwing post holders to mounting posts (P4-1.5-inch to PH4)). Adjust the height of the posts until the top surface of the tube lens bracket is ~50 cm above the surface of the optical table.

55| Position the camera assemblies until the tube lens is in line with the mirror cube (**Supplementary Note 1**, SF6) and the separation between tube lens and mirror cube is ~ 3 mm. Bolt the camera assemblies to the optical table using clamping forks (PF175).

56| Slowly move the diSPIM module away from the coverslip (~5 mm), making sure that the mirror cubes do not touch the tube lenses.

57| Rotate the SPIM arm A camera (along with the tube lens) 45° clockwise and the SPIM arm B camera 45° counterclockwise (looking from the back of the diSPIM system; **Supplementary Note 1**, SF11). Visual alignment as in **Supplementary Note 1**, SF11 is sufficient.

58| Bring the diSPIM module back to the position in Step 46.

59| Switch on both SPIM cameras and open the Hamamatsu HCIMG software. Set the exposure time to 100 ms, use the entire FOV (2,048 × 2,048 pixels) and set the cameras to 'auto intensity' mode. Switch on the 488-nm laser and block the laser input to arm B. Run 'diSPIM Control.vi' using the parameters entered in Step 39. Examine the fluorescence in the SPIM camera B: you should see a horizontal pencil beam (**Supplementary Fig. 3**). If the beam is substantially tilted, adjust the dichroic mirror of SPIM arm A until the beam is horizontal.

60| Unblock the laser input to arm B and you should see a new fluorescence spot caused by epifluorescence close to the pencil beam (in Step 59). If you do not see a fluorescence spot close to the pencil beam, then refer to the Troubleshooting table.
? TROUBLESHOOTING

61| Repeat Steps 59 and 60 for arm B using the readout from SPIM camera A.

62| Bring the focused epifluorescence spot to the center of each SPIM camera chip, either by moving the camera post or by adjusting the mirror cube top plate associated with each camera. This step ensures that the illumination is centered in the SPIM camera.

63| Once the epifluorescence spot is centered in both SPIM cameras, scanning the *Y*-galvo (creating the light sheet) should produce two lines in all three cameras (each line corresponding to a light sheet). Verify this by setting the number of volumes to 1,000 and the light sheet width to 50–80 μm, and by running 'diSPIM Control.vi' in parameter adjustment mode. Two straight lines, corresponding to each beam, should now be visible in the bottom camera (**Supplementary Fig. 4**). In addition, in both SPIM cameras, two lines of fluorescence should be visible: one corresponding to epifluorescence and the second resulting from the excitation induced by the other arm (**Supplementary Fig. 5**).
? TROUBLESHOOTING

PROTOCOL

Adjusting the position of the SPIM objectives using visual feedback from the SPIM and bottom cameras ● TIMING 4–6 h

64| Locate both beams in the bottom camera. The beams should look similar to those displayed in **Supplementary Figure 2**. Move the diSPIM module up-down (over a ~10 μm distance) slowly and examine the relative positions of both beams in the bottom camera. Keep the diSPIM module at the position where both spots are close and of similar size.

65| Scan both light sheets in the Y direction by running 'diSPIM Control.vi' (use the same parameters as in Step 62). In the bottom camera, you should now observe two vertical lines, representing the two light sheets. If the objectives are focused correctly, at the same spot on the coverslip, the two lines should appear as shown in **Supplementary Figure 4**. If the lines are tilted, refer to the Troubleshooting table.
? TROUBLESHOOTING

66| If the lines are displaced vertically relative to each other, adjust the Y-galvo offset for both arms in 'diSPIM Control.vi' so that both lines overlap as viewed in the bottom camera. If the lines are offset in the horizontal direction, bring the diSPIM module down, toward the coverslip, until they overlap. Refer to **Supplementary Figure 4** as necessary.

67| Open the Hamamatsu HCIMG software and run the arm A camera in live mode (exposure time: 100 ms, with autointensity on). By using this camera, two vertical fluorescence lines, one corresponding to the light sheet created by the arm B excitation scanner and the other corresponding to an epifluorescence signal generated by the arm A scanner, should be visible (**Supplementary Fig. 5**).

68| Block the laser input to arm A, and a focused line corresponding to the light sheet produced by arm B should be visible in the arm A camera (**Supplementary Fig. 5**). If this line does not appear in focus, try changing either the offset of the collection objective piezo or the Z-galvo offset corresponding to arm B. The effects of these parameters on the appearance of the beams are shown in **Supplementary Figure 6**.

69| Next, unblock the laser input to arm A. Both SPIM and epifluorescence beams should be visible. If the epifluorescence and SPIM beams are not overlapped, try changing the following parameters in 'diSPIM Control.vi' and rerunning the program: Z-galvo offset of the MEMS mirror of arm B (change in 0.05 V/4 μm steps), offset of the collection objective piezo (change in steps of 0.1 V/2 μm steps) and F-axis position (moving the diSPIM module toward or away from the coverslip in steps of 5 μm). An example of overlapped SPIM and epifluorescence beams is shown in **Supplementary Figure 6**.
▲ **CRITICAL STEP** We recommend changing these parameters serially, and in small increments, while observing their effect using SPIM cameras and the bottom camera. The goal is to observe good overlap between epifluorescence and SPIM beams in each SPIM camera. This ensures that both objectives are focused on the same position.

70| Repeat Steps 67–69 for the other arm. Once both beams overlap in both SPIM cameras, record the Z-galvo offset, Y-galvo offset and objective offset for both arms, as well as the F-axis position.

Centering the region of interest of each SPIM camera ● TIMING 2 h

71| Open the HCIMG program and examine the SPIM beam position in both SPIM cameras. Each SPIM beam should appear to be in the center of its respective FOV, as determined by the Y offset (defined in **Supplementary Note 1**, SF12). If the beams are not centered, adjust the mirror cube using the fine adjustment screws on the top plate of the mirror cube (**Supplementary Note 1**, SF10) until SPIM beams appear centered in both camera FOVs.
▲ **CRITICAL STEP** The Y offset is crucial because the Flash 4.0 camera acquires images in rolling shutter mode, and the speed of acquisition thus depends upon the location of the FOV in the camera chip. The value of Y offset depends on the region of interest (ROI) size. For example, for a 500 × 500 pixel FOV, the Y offset should be 774 pixels and the beam should appear in the middle of the FOV (~1,024 pixels; **Supplementary Note 1**, SF12).

72| Run 'diSPIM Control.vi' in parameter adjustment mode for 1,000 volumes using the parameters recorded in Step 70. As long as the .vi file is running, two vertical lines corresponding to the SPIM beam and epifluorescence beam should be visible in SPIM cameras.

73| Examine the vertical lines in the SPIM cameras using the HCIMG software, and record the X offset position. If the Y offset is lower or higher than 774 (for example, if using a 500 × 500 pixel FOV), adjust the beam position using the fine adjustment screws on the top plate of the mirror cube (**Supplementary Note 1**, SF10).

74| Stop 'diSPIM Control.vi' and record all front panel parameters and SPIM camera offset values. Examine both beams using the bottom camera. Save an image that records the position of the beams in the bottom camera. Future samples should be moved using the *XY* stage until they are located at this beam position, thus ensuring that the light sheets excite the sample and that the sample lies in the FOV of both SPIM cameras.

Imaging a fluorescent bead layer to measure the PSF and beam thickness ● TIMING 1 d
75| *Setting image acquisition parameters for optimal image quality (Steps 75–81).* Place a coverslip with a fluorescent bead layer sample in the sample chamber. Fill the chamber with water and place it on the *XY* stage. Bring the diSPIM module close to the coverslip (F axis position used in Step 74).

76| Select the scouting mode in 'diSPIM Control.vi'. Enter *Z*-Galvo offset, *Y*-Galvo offset and Piezo offset as specified in Step 74. Enter Time/Plane, 5 ms; *Z* Step Size, 0.5 μm; no. of Planes/Volume, 80; Light Sheet Width, 60 μm; no. of Volumes, 1; Time Point Delay, 0; GFP laser Intensity, 5; *Z*-Galvo Conversion factor, 0.013 V; Piezo Conversion factor, 0.05 V.

77| Acquire a single volume by running 'diSPIM Control.vi'.

78| Open up both stacks of tiff images in ImageJ (i.e., corresponding to each view).

79| Examine the maximum intensity projection and individual planes in the volume. Ideally, the beads should appear as shown in **Supplementary Figure 7** (middle) and **Supplementary Data 2** (synch.tif). If beads appear noticeably more blurry, adjust the focus of the collection objectives as follows: set the *Z*-galvo conversion factor in the 'diSPIM Control.vi' to zero, ensuring that the light sheet is stationary (i.e., is not scanned in the *Z* direction). Acquire 1 volume. Examine the stack of tiff images by opening the stack in ImageJ; the image should go from out-of-focus to in focus, and then leave focus again (**Supplementary Data 3**). Next, find the frame at which the beads are in best focus. If the collection objective is in focus, then this frame should be in the middle of the stack. If the focused frame number is more than half the total number of frames, reduce the collection objective offset (in steps of 0.05 V/1 μm); if it is less than half the total number of frames, increase the collection objective offset (in steps of 0.05 V/1 μm). If the bead is not in focus at any frame in the stack, move the diSPIM module toward the coverslip.
▲ CRITICAL STEP Move the diSPIM module in steps of 5 μm. Ensure that the objectives do not touch the coverslip (the bead will appear to 'shake' in the stack if the objectives touch the coverslip). Once the image of the bead appears to go from out-of-focus to in-focus and again out-of-focus, leave the diSPIM module at its current position and adjust the collection objective offset voltage.

80| Enter a *Z*-galvo conversion factor value of 0.013 V in both arms and acquire a volume. Examine individual frames and maximum intensity projections of the bead. Inspect the image stack. If the light sheet lags behind the focus of collection objective (as illustrated in **Supplementary Fig. 7** and **Supplementary Data 2** (lagging.tif)), increase the value of the *Z*-galvo offset (in steps of 0.02 V/1.6 μm). If the light sheet leads the focus of the collection objective (as illustrated in **Supplementary Fig. 7** and **Supplementary Data 2** (leading.tif)), reduce the value of the *Z*-galvo offset (in steps of 0.02 V/1.6 μm). If the maximum intensity projection image looks blurry on its sides but focused in the middle (as shown in **Supplementary Fig. 8** and **Supplementary Data 4**), adjust the *Z*-galvo conversion factor (in steps of 0.001 V). When the *Z*-galvo offset and the *Z*-galvo conversion factor are both optimized, the maximum intensity projection image of the fluorescent bead layer will appear as in **Supplementary Figure 8**.
? TROUBLESHOOTING

81| Repeat Steps 77–80 until a data set in which beads are in focus throughout the stack is obtained (**Supplementary Data 2** (synch.tif)).

82| *Measurement of the PSF (Steps 82–90 and **Fig. 2a**–**c**).* Acquire a volume using the GFP mode of 'diSPIM Control.vi' and parameters obtained in Step 80.
? TROUBLESHOOTING

83| Acquire a background image by blocking the laser and by keeping the parameters the same as in Step 80.

84| Open the stack of images taken in Step 82 in ImageJ.

85| Subtract the average background (background image taken in Step 83) from this stack (Process -> Image calculator).

Figure 2 | Verifying system performance.
(**a**) Measuring the system PSF across the FOV by
collecting a *Z* stack on a fluorescent bead. Light
sheet and the collection objective move in sync.
(**b**) *XY* maximum intensity projections of beads,
showing raw data from view A (left) and view B
(right). Scale bar, 5 μm. (**c**) Higher-magnification
view of beads within dashed rectangular region
in **b**, highlighting the improvement in lateral
and axial resolution after joint deconvolution
procedure. Scale bar, 3 μm. See also
Supplementary Table 4 with lateral and axial
resolution from all beads marked with red circles
in **b**. (**d**) Measuring the light sheet thickness.
The collection objective remains focused on the
fluorescent bead, integrating the fluorescence
as the light sheet is scanned through the bead.
(**e**) Light sheet thicknesses in arm A (blue
diamonds) and arm B (red squares). Apparent
light sheet thicknesses at this location are
2.1 μm (SPIM A) and 1.8 μm (SPIM B).
Data were derived from the bead marked with
the blue squares in **b**. See also **Supplementary Note 1**, SF13, showing the light sheet thickness measured at different locations across the FOV. Note that
schematics **a** and **d** are not to scale; dimensions have been altered to improve image clarity. See also **Supplementary Data 2–5**.
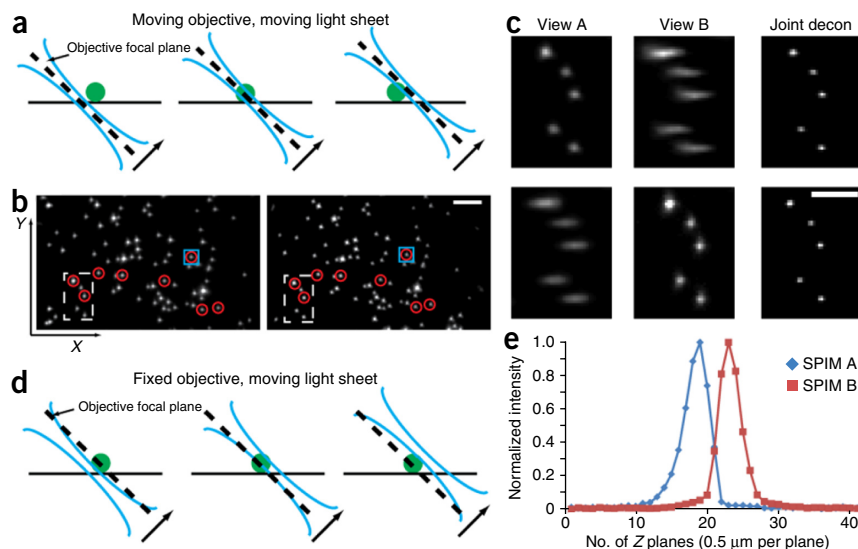
86| Select a bead from this stack (draw a rectangle around the bead, ~14 pixels on a side) and duplicate it in ImageJ
(Image → duplicate).

87| Clear the scale (Analyze → Set scale → click to remove scale).

88| Set the *Z*-scale to 3.07 (0.5/0.1625, i.e., the step size divided by the pixel size (Image → Scale)), so that the voxel
size is isotropic (0.1625 μm in each dimension).

89| Reslice this image from the top (Image → Stack → Reslice).

90| Draw a horizontal line across the center of the bead, and measure the lateral intensity profile of the bead.
Draw a vertical line across the center of the bead and measure the axial intensity profile for the bead (Analyze → Plot
profile). From these intensity profiles, record the full-width at half-maximum (FWHM) values in pixels and convert to μm by
multiplying by 0.1625. These values should be close to 0.5 μm (lateral) and 1.7 μm (axial) (as in **Fig. 2c**, **Supplementary
Table 4** and **Supplementary Data 5** (SPIMA.tif and SPIMB.tif)). These data can be further processed by registering the two
views and performing joint deconvolution to increase resolution, as described in Steps 97–106 (**Supplementary Data 5**
(deconv.tif) and **Supplementary Table 4**).

91| *Light sheet thickness measurement (Steps 91–95 and* **Fig. 2d**,**e***)*. Proper characterization of the light sheet thickness is
important, as the sheet thickness affects the image quality, bleaching, optical sectioning, axial resolution and usable FOV.
Acquire a volume by keeping the collection objective stationary and by sweeping the light sheet through the sample (use
the same parameters as Step 82, except the Piezo conversion factor should be set to zero). The acquired volume should look
similar to **Supplementary Data 6**.

92| Open the image stack in ImageJ.

93| Select an image of a focused bead, and plot the *Z*-axis profile (Image → Stack → Z-axis profile).

94| From the *Z*-axis profile graph, measure the FWHM. Multiply the FWHM by the step size (in this case, 0.5 μm),
thus calculating the thickness of the light sheet.

95| To measure the light sheet thickness across the FOV, keep the parameters the same as in Step 82, but change the
collection piezo offset so that the beads in a different region of the FOV are now in focus. Change the piezo offset and
repeat the light sheet thickness measurement, as described in Steps 91–93. Perform this measurement for 8 or 10 positions

of the collection objective (we recommend varying the collection objective piezo offset in steps of 0.2 V, or 4 µm) so that the sheet thickness is measured for beads located at different X positions in the FOV (examples shown in **Supplementary Note 1**, SF13). After finishing the series of measurements described above, repeat the same procedure for the other SPIM arm. Example results are displayed in **Figure 2** and **Supplementary Note 1**, SF13. The expected light sheet thickness should be close to ~2 µm at the beam waist.

? TROUBLESHOOTING

Imaging cells or *C. elegans* embryos ● TIMING 1–5 d
96| Once the system is assembled and characterized, *C. elegans* embryos (option A) or cultured cells (option B) can be imaged.
(A) Imaging *C. elegans* embryos ● TIMING 4–14 h
  (i) *Embryo isolation.* Add 20 µl of 1% (wt/vol) methyl cellulose solution to a square watch glass.
 (ii) By using the dissecting scope to visualize worms, use the platinum wire worm pick to transfer 5–8 gravid adult *C. elegans* from the worm plate to the drop of methyl cellulose. The adult *C. elegans* should be seen swimming in the methyl cellulose solution.
(iii) Locate a swimming adult and use the scalpel to slice the adult worm in half. Embryos should be seen to spill from the two halves of the adult *C. elegans*.
 (iv) *Transferring embryos to the well chamber.* Place a coverslip into the imaging chamber and pipette 30–40 µl of poly-L-lysine into the center of the coverslip. Wait for ~5 min, and then fill up the chamber with fresh M9 buffer (7–8 ml; **Supplementary Note 1**, SF14).
  (v) Insert the capillary into one end of the aspirator tube (Equipment Setup). Insert a clean 20–200-µl plastic pipette tip into the other end of the aspirator tube. Make sure that only the clean 20–200-µl pipette tip enters the mouth when using the aspirator tube.
 (vi) Place the capillary into the methyl cellulose solution and gently suck several embryos into the capillary via gentle pressure.
(vii) Transfer the tip of the capillary into the imaging chamber. Position the capillary tip so that embryos will fall into the central square of the coverslip.
(viii) Gently expel embryos from the capillary into the imaging chamber. The embryos should fall onto the coverslip and loosely adhere to the poly-L-lysine coating.
 (ix) Position the embryos vertically, so that the long axis of the embryo is perpendicular to the long axis of the coverslip (**Supplementary Note 1**, SF15).
       ▲ CRITICAL STEP Positioning the embryo in this orientation makes it possible to acquire volumetric data with fewer imaging planes, minimizing dose and data processing time while improving acquisition speed.
  (x) Place the imaging chamber on the microscope stage.
 (xi) Use the bottom camera to locate an embryo to be imaged, with the room lights on.
(xii) Bring the embryo to the *XY* stage position recorded in Step 74.
(xiii) Open the LabVIEW program 'diSPIM Control.vi'.
(xiv) Bring the diSPIM module to the *f* axis position recorded in Step 80 by selecting the diSPIM Module Control Mode in 'diSPIM Control.vi' and running 'diSPIM Control.vi'.
 (xv) Once the diSPIM module moves to this *F*-axis position, select 'scouting mode' and enter the parameters from Step 80, except set the *Z* Step Size to 1 µm and the number of Planes/Volume to 50.
(xvi) Set the ROI of each SPIM camera as in Step 73.
(xvii) Acquire one volume. Open the volume in ImageJ. Verify that the embryo is in the FOV. If the embryo is not in the FOV (either in one or both SPIM cameras), translate the *XY* stage slowly. After each move, acquire a volume and examine it in ImageJ to check the embryo position. The goal is to center the embryo in both SPIM cameras' FOVs.
(xviii) Ensure that the light sheet is covering the entire embryo. If this is not the case, change the *Y*-galvo offset of the arm (in steps of 0.1 V/8 µm) causing incomplete illumination, until the entire embryo is illuminated (**Supplementary Fig. 9** and **Supplementary Video 3**).
(xix) Make sure that the image stack corresponding to each view covers the entire embryo (as shown in **Supplementary Fig. 9** and **Supplementary Video 3**). If part of the embryo is located outside the imaging stack, move the diSPIM module up and down (in steps of 5 µm). Acquire an imaging volume each time the diSPIM module is moved, checking the embryo coverage. Stop when the embryo is contained within the stack. Open the stack and examine it in ImageJ.
       ▲ CRITICAL STEP Do not change the *Z* offset of the MEMS mirror, as this will alter synchronization between the detection piezo and MEMS mirror. Changing the *Z*-offset value could also alter the overlap between two arms.
 (xx) Acquire 1 volume in each view and open the resulting image stack in ImageJ.

Figure 3 | Imaging labeled histones in a *C. elegans* embryo with diSPIM. Selected maximum intensity projections from ~14-h imaging experiment, showing nuclear histones in a living *C. elegans* embryo. Data indicate the isotropic resolution expected from a properly functioning diSPIM system, as well as the ability to image samples over many time points with negligible bleaching and photodamage. Time is indicated as hours post fertilization (h.p.f.) in h:min:s format. See also **Supplementary Video 1**, **Supplementary Data 1** and **7**.

(xxi) Examine the individual planes and the volumes corresponding to each view. If the images appear blurry in either view, adjust the relevant collection objective offset (in steps of 1 μm) until the images appear sharp.

(xxii) Examine the maximum intensity projections produced by each camera. These images should look similar to those shown in **Supplementary Figure 10** (see also **Supplementary Video 4**). Compare the volumes collected by the diSPIM arms. If the difference in signal intensity between the two arms is >20%, refer to the TROUBLESHOOTING section. If the same information is captured within both volumes, the system is ready to acquire an extended time series. Now take a background image by setting the laser intensity to zero and acquiring a volume.
? TROUBLESHOOTING

(xxiii) Run 'diSPIM Control.vi' in Image Acquisition Mode (GFP, 488 nm) with the following parameters for 14-h imaging: number of Volumes, 1,000; Time Point Delay, 60 s, and provide a file name. Note that we assume that imaging commences when the embryo is in the 4–8-cell stage.

(xxiv) Process the images according to the instructions in Steps 97–106. **Figure 3** shows selected maximum intensity projections from the deconvolved data set (see **Supplementary Data 7** for data relating to this figure); see also **Supplementary Data 1**.

(B) Imaging cells ● TIMING 4–5 d

(i) *Preparing the coverslips for cellular imaging.* Place rectangular glass coverslips in a glass beaker half-filled with distilled water, taking care to separate coverslips that are stuck together. Boil them for 10 min. Let the solution cool and occasionally agitate.

(ii) Rinse the coverslips extensively with distilled water.

(iii) Transfer the coverslips to a clean glass beaker with 1 M HCl solution. Place them in a fume hood and allow them to stand overnight.

(iv) The next day, rinse them extensively with distilled water.
▲ **CRITICAL STEP** All procedures from this point should be performed in a tissue culture hood using routine aseptic conditions.

(v) Transfer the coverslips with a stainless steel pair of forceps to a new clean beaker with 50% (vol/vol) ethanol solution. Agitate occasionally for 1 h. Subsequently, transfer the coverslips to a 70% (vol/vol) ethanol solution, immerse them for 30 min and finally transfer them to a 90% (vol/vol) ethanol solution and immerse the coverslips overnight.

(vi) *Cell plating and transfection.* Before cell plating, place the coverslips in a 100-mm tissue culture dish (one dish can fit up to two rectangular coverslips) in a tissue culture hood using autoclaved stainless steel forceps.
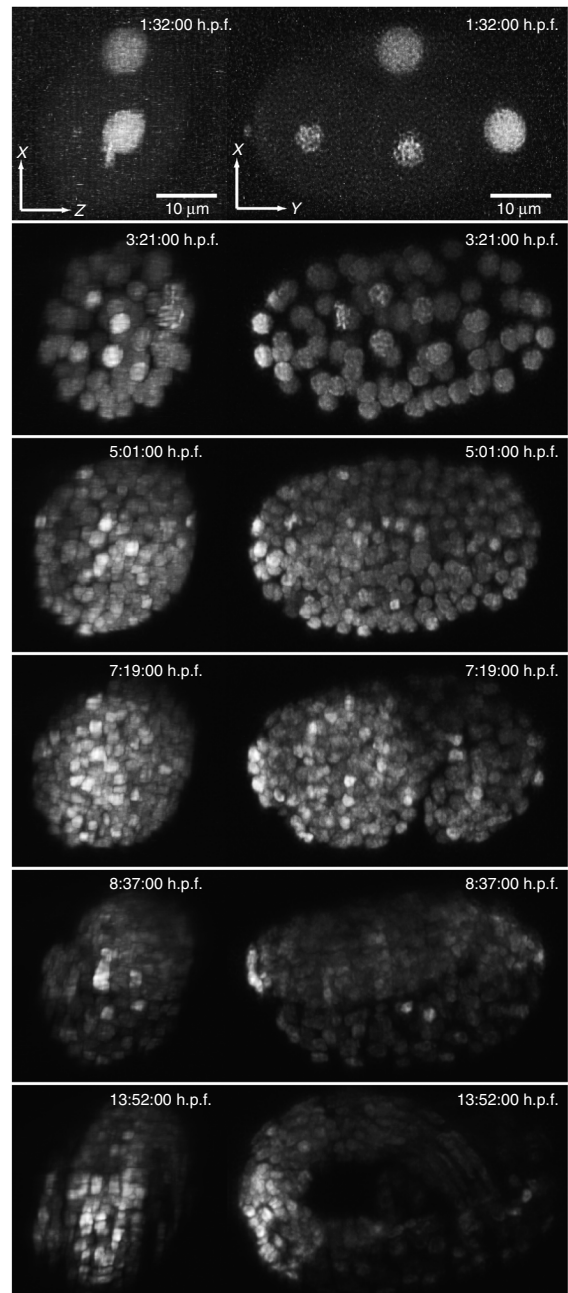▲ **CRITICAL STEP** Let the coverslips air-dry in the dish before cell plating.

Figure 4 | Imaging GFP-tagged Harvey rat sarcoma viral oncogene homolog (HRAS) in transformed human lung fibroblast cells with diSPIM. (**a**) *XY* maximum intensity projection from 351 time-point volumetric series. (**b**) *XZ* maximum intensity projection to accompany **a**. (**c**) Single *XZ* slice, highlighting membrane ruffling and infolding. Data are shown at 15-s intervals, but note that acquisition occurred every 5 s, demonstrating the capability of diSPIM to capture fast cellular events at high spatial resolution. (**d**) Long-term reorganization of the plasma membrane, indicating growth and remodeling of filopodial protrusions. These images were rendered using the 'Hot Red' lookup table in ImageJ. Scale bars, 5 µm. See also **Supplementary Video 2** and **Supplementary Data 8**.
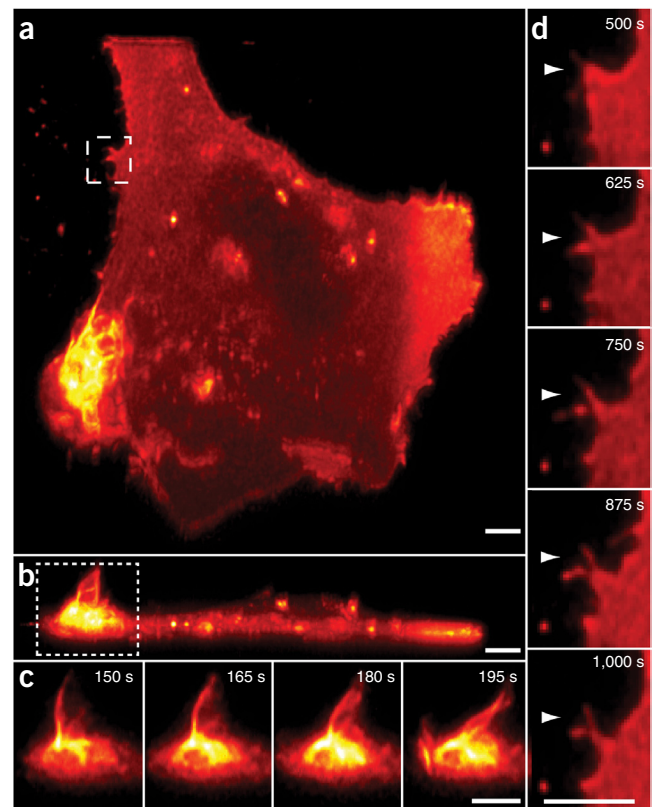
(vii) Trypsinize the cells according to standard procedure. Add serum to deactivate trypsin. Pipette and transfer the mixture to 15-ml sterile centrifuge tubes. Resuspend the mixture in complete medium (DMEM plus 10% (vol/vol) FBS, in this case) and plate on coverslips.

(viii) The next day, inspect the cells under a phase-contrast microscope; make sure that the cells have adhered well and that the confluency is between 50 and 80%. Before setting up the DNA-lipid complexes for transfection, replace the medium in the cell culture dishes with warmed (37 °C), fresh medium supplemented with 5% (vol/vol) FBS instead of the previous 10% (vol/vol) FBS medium.

(ix) Pipette 500 µl of plain DMEM in a sterile 1.5-ml tube. Add 5–10 µg of plasmid DNA (GFP-tagged H-Ras), and mix it well but gently.

▲ **CRITICAL STEP** Plasmid DNA should be of high purity to increase transfection efficiency and to minimize toxicity.

(x) Add TurboFect liposomes reagent at a 2:1 or 3:1 liposome:DNA ratio and mix four or five times gently. Let it stand for 15–20 min.

(xi) Distribute the transfection mix to the cells dropwise using a 1-ml pipette (the broad tip reduces the disruption of lipid-DNA complexes).

(xii) Return the cells to the incubator (37 °C, 5% CO_2) overnight.

(xiii) *Cellular imaging.* On the next day, inspect the cells on a tissue culture microscope for toxicity. Only healthy-looking cultures should be used for imaging.

(xiv) Inspect the cells under an inverted epifluorescence microscope for the expression of the construct.

(xv) Replace the medium with prewarmed phenol red–free DMEM supplemented with high glucose (to 4.5 g per liter), GlutaMAX (to 2 mM), pyruvate (to 1 mM), sodium bicarbonate (to 3.7 per liter), HEPES (to 5 mM) and 10% (vol/vol) FBS. Allow the cells to equilibrate in the tissue culture incubator (37 °C, 5% CO_2), for 1–2 h before imaging.

(xvi) Place the coverslips with the cells inside the imaging chamber, and assemble as shown in **Supplementary Note 1**, SF4. Gently cover the cells with imaging medium as described in Step 96B(xv).

(xvii) Open 'diSPIM Control.vi'.

(xviii) Locate a cell using the bottom objective and position it at the *X* and *Y* pixel location recorded in Step 74 by translating the sample appropriately with the *XY* stage.

(xix) Bring the diSPIM module close to the coverslip (*F* axis position: recorded in Step 80) by running 'diSPIM Control.vi' in diSPIM module control mode.

(xx) Enter the same front panel parameters as in Step 80.

(xxi) Acquire a volume by running 'diSPIM control.vi' in scouting mode, and examine the image stack in ImageJ.

(xxii) Ensure that the ROI in the cell is captured within the imaging volume, by examining the maximum intensity projection and individual images within the stack. If the cell is not captured within the imaging volume, either translate the *XY* stage or increase the number of planes per volume (up to 75, assuming 1-µm steps) and recapture the volume. Repeat until the ROI is captured within the image stack.

(xxiii) If the images appear blurry, adjust the collection objective offset of that arm in small steps (0.05 V, corresponding to 1 µm).

(xxiv) Once both views are optimized, start time-lapse imaging by running the 'diSPIM Control vi' in 'Image Acquisition (GFP, 488 nm)' mode. Enter the number of volumes and time delay between volumes on the basis of your requirements (for the data in **Fig. 4** and **Supplementary Data 8**, the number of volumes was 350 and the time delay 5 s).

(xxv) Process the acquired images as described in Steps 97–106 below.

Data processing ● TIMING 3–8 h

97| The data files output from each SPIM camera should be in multipage TIFF format—i.e., each TIFF file should contain an entire volume represented as a stack of individual planes (images). Separate all volume files into two folders, corresponding to the two SPIM cameras, as shown in **Supplementary Note 1**, SF16.

98| Crop and subtract the dark background from all volume files (an example ImageJ macro is provided as **Supplementary Note 3**).

99| Navigate to http://mipav.cit.nih.gov/download.php, fill out the request form and download the most recent 64-bit version of MIPAV 7.1.0. Note that Steps 99–101 are only performed during installation and setup of MIPAV.

100| Install MIPAV and allocate memory according to the instructions provided in the MIPAV installation guide: http://mipav.cit.nih.gov/pubwiki/index.php/Installing_mipav. When MIPAV runs for the first time, specify the amount of memory available (minimal requirement is 2 GB). Note that MIPAV can take full advantage of the memory resources available in the computer. For more information on MIPAV's memory allocation, users can refer to http://mipav.cit.nih.gov/pubwiki/index.php/Allocating_Memory_in_MIPAV (the Java programming language does not currently allow array indices larger than 2,147,483,647, but this restriction should be removed with the release of JDK 9 in 2015).

101| Install the diSPIM plug-in. In the MIPAV program, click 'Plugins' in the menu bar, thus popping up the dialog box 'Install Plugin'. Browse the working dictionary of MIPAV, and select 'PlugInGenerateFusion.class' for installation, as shown in **Supplementary Note 1**, SF17. Reclick 'Plugins' in the menu bar, click 'SPIM' and choose 'Generate Fusion', which generates the diSPIM dialog box. The current version of the plug-in is 'generate fusion 544e'.

102| Set the correct parameters for registration of the two views. In the diSPIM dialog box, select the 'File' tab, as shown in **Supplementary Note 1**, SF18. Under the 'File information' subheading, there are three options: 'No registration', 'One time registration' or 'All time registration' (see the red ellipses in the figures). If users perform the registration with third-party software, they can choose 'No registration' and import the relevant registration matrix file that is produced from the third-party software. This matrix will be applied to all time points. Choosing 'One time registration' means that users need to specify the volumetric time point from which to perform the registration, and to specify the directory in which to save the transformation matrix after registration. If the sample does not move much during imaging, an early time point can be used to generate a registration matrix that is applicable to the entire time course. In such cases, we usually choose one of the first 20 time points for matrix generation. In samples in which substantial movement occurs during imaging, it is necessary to process the data in subgroups (we have found that subgroups consisting of ~100 time points work well), or even run registrations at each time point in the series by choosing 'All time registration'. In the latter case, users will only need to specify the directory in which to save the matrix for each time point.

103| After setting the registration parameters, define the range of angles used when transforming volume B into volume A via the registration procedure. Typically, a searching angle range from −10° to 10°, a coarse angle increment of 2°–3° and a fine-angle increment of 0.5°–1° results in an acceptable registration within 5–10 min.

104| Specify where the raw data are located (**Supplementary Note 1**, SF18). Images placed in the 'transform' directory will be rotated by 90° about the *Y* axis (as illustrated in **Supplementary Note 1**, SF19), transforming them into the coordinate system of the images inside the 'base' directory. Also specify the range of volumes that need to be transformed, fused and deconvolved. If this range is left empty, the plug-in will automatically select all volumes.

105| Set parameters in the 'Option' tab (**Supplementary Note 1**, SF20), including pixel size and the number of concurrent fusions to run (at most, the number of CPU cores on the machine). Users also need to set other options by selecting the 'Options' tab in the plug-in, as shown in **Supplementary Note 1**, SF20. In the 'algorithm options' (red box), set the image pixel size and the number of concurrent fusions, which depend on the number of CPU cores (e.g., users can input up to 12 if the computer has 12 CPU cores). If desired, specify whether to display or to save intermediate processing steps, such as maximum intensity projections or fusions based on the arithmetic or geometric mean between the two views. Finally, set the

GPU-based deconvolution parameters including iteration number (at least 10), sigma values (in pixels) of the PSF characterizing each view (typically 3.5, 3.5 and 9.6 for X, Y, and Z in the base view; 9.6, 3.5, and 3.5 for X, Y, and Z in the transformed view) and the directory to save the images after deconvolution.
▲ CRITICAL STEP The computer may run out of memory if you display pre-fusion images, the arithmetic mean and the geometric mean while the registration program is running. We recommend saving these images and examining them once the processing is completed. When the computer runs out of memory, the indicator on the MIPAV toolbar showing the memory being used will turn red.

106| *Confirm operations*. Once all parameters are set, click the 'OK' button and check the pairs of base and transformed image stacks that pop up (**Supplementary Note 1**, SF21). If all are correct, click 'Yes' to run the joint deconvolution.
? TROUBLESHOOTING

? TROUBLESHOOTING
Troubleshooting advice can be found in **Table 1**.

TABLE 1 | Troubleshooting table.

Step	Problem	Possible reason	Solution
29	Beams are not intersecting	Scanner is not mounted properly	Remount the scanner and recheck beam intersection
		Dichroic mirror is not placed properly	Adjust the dichroic filter cube using fine alignment screws (shown in SF5 in **Supplementary Note 1**) until the beams intersect
60	Epifluorescence spot is not close to the pencil beam	Objectives are not focused at same spot	Adjust the position of the objectives coarsely (as in Step 46) until both focus at the same spot
		Y offset of the MEMS mirror (Y-galvo offset) is not optimal	Change the Y offset of the MEMS mirror (either arm or both arms) to bring the epifluorescence spot closer to the pencil beam
63	In the SPIM camera, only one line is visible	This signifies that both objectives are co-focused and well aligned	To test alignment, move the diSPIM module up or down (5–10 μm); two lines should be visible
65	Light sheet is tilted (shown in **Supplementary Fig. 4**)	Scanner does not make a 45° angle with respect to the optical table	Rotate the scanner that is creating the light sheet so that lines appear vertical in the bottom camera
80	Maximum intensity projection of beads image is blurry	Collection objective is not focused	Change the collection piezo offset
		Light sheet and collection objectives are not synchronized	Change the Z-galvo conversion factor
		Z-galvo offset is not optimal	Change the Z-galvo offset
		Light sheet is thicker than it should be	Measure the light sheet thickness
		Beads in the sample are aggregated	Find single beads, make another sample if necessary

(continued)

TABLE 1 | Troubleshooting table (continued).

Step	Problem	Possible reason	Solution
82	Beads appear to shake during acquisition	Optical table is not floating properly	Re-float the optical table
		Objectives are touching the coverslip	Move the diSPIM module up
		Objectives are touching the side walls of the chamber	Move the *XY* stage
		Sample chamber is not placed properly	Remount the sample chamber carefully
		Camera is not mounted properly	Ensure that the posts bolting down the camera are secure
95	Light sheet is thicker than it should be (as determined after measuring sheet thickness)	diSPIM module is not at the optimal position	Move the diSPIM module (in steps of 5 μm) and repeat the measurement
		Objective creating the sheet is not at the optimal position	Move the objective (in steps of 5 μm) and repeat the measurement
		Iris is stopped down too tightly	Open the iris
96A(xxii)	The embryo cannot be seen in SPIM images	Embryo is not in the FOV of SPIM cameras	Move the *XY* stage and bring the embryo into the FOV
		The horizontal offset of the SPIM camera is wrong	Check the horizontal offset of the SPIM camera by running the camera in live mode in room light using HCIMG software
		Laser is off	Ensure that the laser is on when data is acquired
		Embryo is not attached to the coverslip and is moving around	Ensure that the embryo is attached to the coverslip and does not move, This can easily be monitored using the bottom camera
106	Processed data have artifacts or the quality of images is suboptimal	Raw data are not good	Check the raw data and make sure that both views are equally good
		Registration is not optimal	Check the transformed image and make sure that registration is good (examples are shown in **Supplementary Note 1**, SF1). Also consider breaking up the registration as described in Step 102
		X, *Y*, *Z* resolution parameters entered into processing software are incorrect	Check the *X*, *Y* and *Z* resolution parameters entered in MIPAV
		Deconvolution parameters are wrong	Check the deconvolution parameters in MIPAV

● **TIMING**
Steps 1–10, setting up the computer, optical table and excitation laser sled and testing: 2 d
Steps 11–20, setting up the diSPIM imaging frame and installing the lower imaging path: 4–6 h
Steps 21–24, aligning the excitation scanners: 3–4 h
Steps 25–29, assembling optics for dichroic filter cube holder and attaching them to excitation scanners: 1 h

Steps 30–48, assembling objective piezo assemblies and coarsely aligning SPIM objectives: 1 d
Steps 49–63, assembling and positioning SPIM cameras: 4–5 h
Steps 64–70, adjusting the position of the SPIM objectives, using visual feedback from the SPIM and bottom camera: 4–6 h
Steps 71–74, centering the ROI for each SPIM camera: 2 h
Steps 75–95, imaging fluorescent beads to measure PSF and light sheet thickness: 1 d
Step 96A: embryo preparation and imaging: 4–14 h
Step 96B: cell preparation and imaging: 4–5 d
Steps 97–106, data processing: 3–8 h

ANTICIPATED RESULTS

If this protocol is followed carefully, the user should expect data of similar quality to **Figures 2**–**4** and **Supplementary Videos 1** and **2**. As an additional guide, we provide supplementary data of volumetric stacks corresponding to the following:

• Raw bead data acquired from each arm and the resulting deconvolution (**Supplementary Data 5**)
• An example of raw embryo data acquired from each arm and the resulting deconvolution (corresponding to **Fig. 3** and **Supplementary Data 7**)
• An example of misregistered embryo data and the resulting low-quality deconvolution (**Supplementary Data 1**)
• An example of raw cellular data acquired from each arm and the resulting deconvolution (corresponding to **Fig. 4** and **Supplementary Data 8**)

1. Voie, A.H., Burns, D.H. & Spelman, F.A. Orthogonal-plane fluorescence optical sectioning: three-dimensional imaging of macroscopic biological specimens. *J. Microsc.* **170**, 229–236 (1993).
2. Fuchs, E., Jaffe, J.S., Long, R.A. & Azam, F. Thin laser light sheet microscope for microbial oceanography. *Opt. Express* **10**, 145–154 (2002).
3. Huisken, J., Swoger, J., Del Bene, F., Wittbrodt, J. & Stelzer, E.H.K. Optical sectioning deep inside live embryos by selective plane illumination microscopy. *Science* **305**, 1007–1009 (2004).
4. Holekamp, T.F., Turaga, D. & Holy, T.E. Fast three-dimensional fluorescence imaging of activity in neural populations by objective-coupled planar illumination microscopy. *Neuron* **57**, 661–672 (2008).
5. Wu, Y. *et al.* Inverted selective plane illumination microscopy (iSPIM) enables coupled cell identity lineaging and neurodevelopmental imaging in *Caenorhabditis elegans*. *Proc. Natl. Acad. Sci. USA* **108**, 17708–17713 (2011).
6. Keller, P.J., Schmidt, A., Wittbrodt, J. & Stelzer, E.H.K. Reconstruction of zebrafish early embryonic development by scanned light sheet microscopy. *Science* **322**, 1065–1069 (2008).
7. Tomer, R., Khairy, K., Amat, F. & Keller, P.J. Quantitative high-speed imaging of entire developing embryos with simultaneous multiview light-sheet microscopy. *Nat. Methods* **9**, 755–763 (2012).
8. Krzic, U., Gunther, S., Saunders, T.E., Streichan, S.J. & Hufnagel, L. Multiview light-sheet microscope for rapid *in toto* imaging. *Nat. Methods* **9**, 730–733 (2012).
9. Planchon, T.A. *et al.* Rapid three-dimensional isotropic imaging of living cells using Bessel beam plane illumination. *Nat. Methods* **8**, 417–423 (2011).
10. Gao, L. *et al.* Noninvasive imaging beyond the diffraction limit of 3D dynamics in thickly fluorescent specimens. *Cell* **151**, 1370–1385 (2012).
11. Wu, Y. *et al.* Spatially isotropic four-dimensional imaging with dual-view plane illumination microscopy. *Nat. Biotechnol.* **31**, 1032–1038 (2013).
12. Swoger, J., Verveer, P., Greger, K., Huisken, J. & Stelzer, E.H.K. Multi-view image fusion improves resolution in three-dimensional microscopy. *Opt. Express* **15**, 8029–8042 (2007).
13. Temerinac-Ott, M. *et al.* Multiview deblurring for 3D images from light-sheet-based fluorescence microscopy. *IEEE Trans Image Process.* **21**, 1863–1873 (2012).
14. Pitrone, P.G. *et al.* OpenSPIM: an open-access light-sheet microscopy platform. *Nat. Methods* **10**, 598–599 (2013).
15. Gualda, E.J. *et al.* OpenSpinMicroscopy: an open-source integrated microscopy platform. *Nat. Methods* **10**, 599–600 (2013).
16. Capoulade, J., Wachsmuth, M., Hufnagel, L. & Knop, M. Quantitative fluorescence imaging of protein diffusion and interaction in living cells. *Nat. Biotechnol.* **29**, 835–839 (2011).
17. Gao, L., Shao, L., Chen, B.C. & Betzig, E. 3D live fluorescence imaging of cellular dynamics using Bessel beam plane illumination microscopy. *Nat. Protoc.* **9**, 1083–1101 (2014).
18. Huisken, J. & Stainier, D.Y.R. Even fluorescence excitation by multidirectional selective plane illumination microscopy (mSPIM). *Opt. Lett.* **32**, 2608–2610 (2007).
19. Silvestri, L., Bria, A., Sacconi, L., Iannello, G. & Pavones, F.S. Confocal light sheet microscopy: micron-scale neuroanatomy of the entire mouse brain. *Opt. Express* **20**, 20582–20598 (2012).
20. McAuliffe, M.J. et al. Medical image processing, analysis, and visualization in clinical research. *Proceedings of the 14th IEEE Symposium on Comput. er-Based Medical Systems (CBMS '01)* **381** (2001).
21. Stiernagle, T. Maintenance of *C. elegans*. in *WormBook* (ed. The *C. elegans* Research Community) doi:10.1895/wormbook.1.101.1 (11 February 2006).
22. York, A.G. *et al.* Instant super-resolution imaging in live cells and embryos via analog image processing. *Nat. Methods* **10**, 1122–1126 (2013).
23. Murray, J.I. & Bao, Z. in *Imaging in Developmental Biology: A Laboratory Manual* Vol. 56 (eds. Sharpe, J. & Wong, R.) (Cold Spring Harbor Laboratory, 2010).
24. Shroff, H. *et al.* Dual-color superresolution imaging of genetically expressed probes within individual adhesion complexes. *Proc. Natl. Acad. Sci. USA* **104**, 20308–20313 (2007).